Design of dimpled engineering surfaces for improving lubrication performance in rolling-sliding contacts

Fukuo Hashimoto* and Rao S. Zhou

Advanced Finishing Technology Ltd.,
3804 Heron Watch Dr., Akron OH 44319, USA
Email: fukuo@advancedfinishingtechnology.org
*Corresponding author

Abstract: Functional performance depends largely on the surface characteristics of critical components. This paper describes the design of dimpled engineering surfaces and the fabrication of micro-patterns on steel samples. The designed engineering surfaces are analysed and evaluated in terms of their mixed EHL film thicknesses and pressure distributions in the elliptical Hertzian contact zone.

Keywords: surface engineering; surface structuring; surfaces; mixed EHL contact; film thickness; dimpled surfaces; finishing technology.

Reference to this paper should be made as follows: Hashimoto, F. and Zhou, R.S. (2017) 'Design of dimpled engineering surfaces for improving lubrication performance in rolling-sliding contacts', *Int. J. Abrasive Technology*, Vol. 8, No. 1, pp.44–54.

Biographical notes: Fukuo Hashimoto is the President and Chief Scientist of AFT (Advanced Finishing Technology Ltd.) and was a Senior Scientist and the Director of The Timken Company. He joined The Timken Company in 1988, and retired in 2015. He received his Doctoral degree from the University of Tokyo in 1984. He completed the SEP program at Stanford University in 2000. He is a fellow member of the International Academy for Production Engineering (CIRP) and a past Chairman of CIRP STC-G (Grinding Academy). He also is a fellow member of SME (the Society of Manufacturing Engineering).

Rao S. Zhou is a Scientist (retired) of The Timken Company and a world-class expert in tribology research. He obtained his PhD in Mechanical Engineering from the Northwestern University and has published numerous papers for the Society of Tribology and Lubrication Engineers (STLE). He is the co-inventor, with Fukuo Hashimoto of the innovative isotropic finishing process and axial motor integrated package bearings.

This paper is a revised and expanded version of a paper entitled 'Design of dimpled engineering surfaces for improving lubrication performance in rolling-sliding contacts' presented at ISAAT2017, Okinawa, 3–6 December 2017.

1 Introduction

The functional performance of critical mechanical components depends on the characteristics represented by surface roughness, surface texture and surface integrity (Hashimoto et al., 2016a), in addition to geometrical accuracy. In general, functional surfaces are refined by abrasive fine-finishing technology after undergoing grinding or hard-turning processes. Each abrasive fine-finishing process provides its own unique surface texture and integrity; thus, the selection of the fine-finishing method becomes crucial for achieving the required level of performance (Hashimoto et al., 2016b).

Heavily loaded mechanical components, such as bearing rolling elements, work under mixed lubrication contacts where the surface roughness and the lubricant film thickness are of the same order of magnitude (Patir and Cheng, 1978). Therefore, the surface characteristics of the components significantly affect lubrication performance, which in turn determines product performance in areas such as service life, friction force, wear, heat generation, etc. (Zhou and Hashimoto, 1995). Although the components' surface characteristics are adequately managed by the abrasive finishing process, applying an enhanced finishing process – in the form of an artificial engineering surface designed to achieve specific desired surface characteristics – adds greater value with performance superior to current products.

In this paper, the fabrication of steel samples with micro-pattern surfaces is described, as is the design of various dimpled engineering surfaces with different shapes and arrangements. The elastohydrodynamic lubrication (EHL) contacts of the designed surfaces are simulated in order to evaluate lubrication performance (Zhu and Hu, 1999, 2001; Hu and Zhu, 2000; Liu et al., 2006). Also, the lubrication performance of the dimpled surfaces is compared to that of perfectly smooth surfaces. Finally, this paper establishes the design criteria for optimising dimpled surfaces as the basis of surface structuring technology (Evans and Bryan, 1999).

2 Model description

The mixed EHL model is well developed and can accurately simulate the mixed lubrication of engineering surfaces. It handles a wide range of operating conditions (Zhu and Hu, 1999, 2001; Hu and Zhu, 2000; Liu et al., 2006). In this study, the model is employed to simulate the EHL film thickness of engineered surfaces under various operating conditions.

The fluid pressure distribution in the contact domain can be expressed by the following Reynolds equation:

$$\frac{\partial}{\partial x}\left(\frac{\rho}{12\eta}h^3\frac{dp}{dx}\right)+\frac{\partial}{\partial y}\left(\frac{\rho}{12\eta}h^3\frac{\partial p}{\partial y}\right)=U\frac{\partial(\sigma h)}{\partial x}+\frac{\partial(\rho h)}{\partial t} \tag{1}$$

where the x coordinate coincides with the motion direction, U is the rolling-sliding speed.

The instantaneous lubricant film thickness h between two surfaces is calculated by the following geometric equation:

$$h=h_0(t)+\frac{x^2}{2R_x}+\frac{y^2}{2R_y}+V(x,y,t)+\delta_1(x,y,t)+\delta_2(x,y,t) \tag{2}$$

where h_0 is the nominal film thickness. R_x and R_y are the local radii of curvature in the x and y directions, respectively. δ_1 and δ_2 denote the micro roughness amplitude of surfaces 1 and 2 and V is the surface deformation, which is computed by the following integral:

$$V(x, y, t) = \frac{2}{\pi E'} \iint_{\Omega} \frac{p(\xi, \varsigma)}{\sqrt{(x-\xi)^2 + (y-\varsigma)^2}} d\xi d\varsigma \tag{3}$$

In this paper, a non-Newtonian model is used and the flow factors φ_x, φ_y (Patir and Cheng, 1978) and the lubricant properties are calculated. Also, the viscosity η at low share rate is calculated by the Barus equation:

$$\eta = \eta_0 \exp(\alpha p) \tag{4}$$

The lubricant density as a function of pressure is described by the Dowson-Higginson formula (Dowson and Higginson, 1966):

$$\rho = \rho_0 \left(1 + \frac{0.6 \times 10^{-9} p}{1 + 1.7 \times 10^{-9} p} \right) \tag{5}$$

3 Surfaces and contact conditions

In tapered roller bearings, the spherical profile of the roller end contacts the flange surface (rib) of the inner ring (cone). The rib-roller end contact zone is elliptical under rolling-sliding conditions. This paper simulates the elliptical EHL interfaces. Figure 1(a) illustrates the rolling-sliding contact of two rolling element bodies. The upper surface is a perfectly smooth reference surface with a rolling speed U1 and the bottom surface is a tested surface with a rolling speed U2. The slide-to-roll ratio (SR ratio) is defined as 2(U2 – U1) / (U2 + U1). For positive SR ratios, U2 > U1 and for negative SR ratios, U2 < U1. Figure 1(b) shows the rib-roller contact with a longitudinal ellipse along the motion direction. The input parameters and operating conditions are summarised in Table 1.

Table 1 Input parameters and operating conditions

Parameter		*Symbol*	*Value*
Contact geometry	Effective radii	Rx	810.78 mm
		Ry	106.56 mm
	Ellipse condact	Major axis a	1.4 mm
		Minor axis b	0.370 mm
		Ellipticity k = b/a	0.2643
Elastic modulus		E	230.77 Gpa
Applied normal load		W	228 N
Maximum Hertzian pressure		P_H	0.21 Gpa
Lubricant	Mineral oil	Viscosity η_0	0.006278 Pa s
	Pressure-viscosity exponent	α	19.36/Gpa
Entraining speed		U	0.15, 2, 12 m/s
Slide-to-roll ratio		S	0.25

Figure 1 Rolling-sliding contact of two rolling bodies, (a) rolling-sliding contact (b) elliptical contact zone

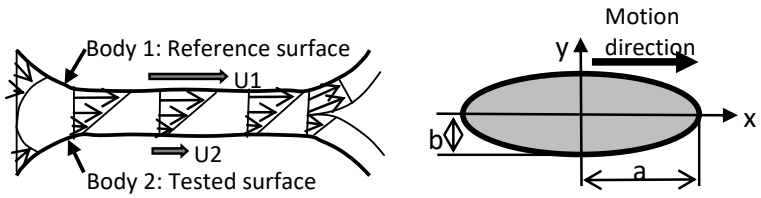

(a) (b)

Note: Rib-roller end contact in tapered roller bearings.

4 Fabrication of dimpled engineering surfaces

Photolithography and chemical etching methods are applied to make micro-pit patterns on hardened steel material. Figure 2 shows the sequence of the fabrication of the dimpled engineering surface. A steel plate (52100, HRC62, 25 mm × 25 mm) is used with a photo-resistant coating (polyamide) of about 1.6 μm in thickness. Micro-patterns are drawn on a glass plate and then exposed to ultraviolet light for one minute. The etching is conducted with nitrohydrochloric acid (10 mol/l HCI: 10 mol/l HNO_3 = 3:1) for four minutes. The fabricated steel samples with the resulting dimpled engineering surfaces are shown in Figure 3.

Figure 2 Fabrication processes of dimpled engineering surfaces on hardened steel material (see online version for colours)

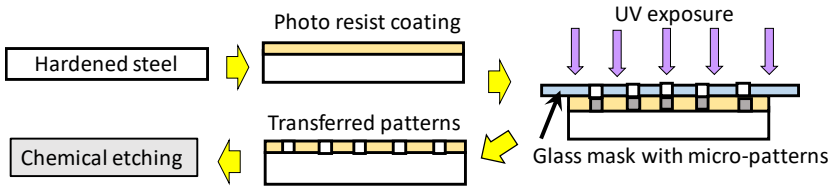

Figure 3 Samples of dimpled engineering surfaces created on hardened steel plates, (a) circular dimples (ϕ6 μm, depth 1 μm) (b) elliptical dimples (12 μm × 2 μm, depth 1 μm)

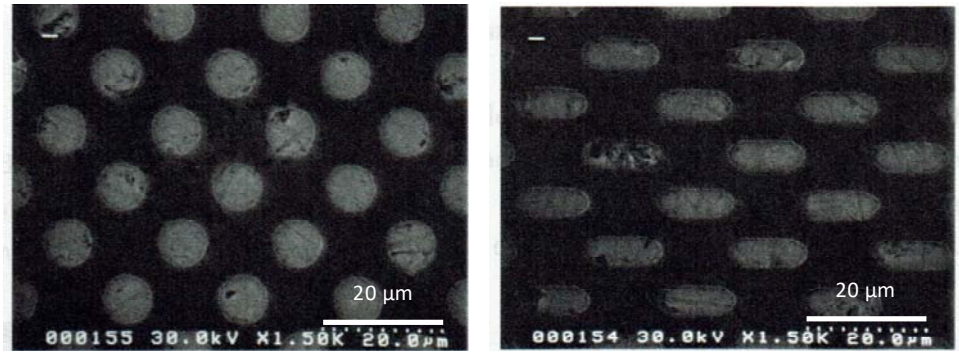

(a) (b)

Table 2 Design of dimpled engineering surfaces and results of mixed EHL analysis

Category	*Geometrical parameters for engineered surface design*									*Performance on rolling-sliding contact*		
		Dimple dimensions				*Dimple row distance*		*Dimple area*		*Average film thickness*	*Contact load ratio*	*λ ratio*
Cases	*Dimple arrangement*	*d*	*e*	*f*	*t*	*j*	*k*					
		μm	*μm*	*μm*	*μm*	*μm*	*μm*	*%*		*nm*	-	-
1	Gigzag	-	48	24	1	72	24	26.2		138.6	0.193	0.521
2	Regular	-	48	24	1	72	48	26.2		134.4	0.165	0.508
3	Gigzag	36	-	-	1	60	30	26.2		133.9	0.445	0.49
4	Regular	36	-	-	1	60	60	26.2		139.1	0.261	0.511
5	Gigzag	-	24	48	1	24	72	26.2		127.7	0.385	0.48
6	Regular	-	24	48	1	48	72	26.2		128.6	0.364	0.486
7	Regular	-	24	48	1	96	144	6.6		288.4	0	2.003
8	Regular	-	24	48	1	192	144	3.3		232.5	0	2.253
9	Regular	-	12	24	1	96	144	1.6		211.6	0	2.867
10	Regular	-	48	96	1	96	144	26.2		167.8	0.124	0.635
11	Regular	-	24	48	0.5	96	144	6.6		219.2	0	3.048
12	Regular	-	24	48	2	96	144	6.6		224.6	0	0.775
Smooth	-	-	-	-	-	-	-	0		239.5	0	-

5 Design of dimpled engineering surfaces

Figure 4 denotes the dimensions of the dimples. Circular and elliptical dimples are created with flat bottoms in which the depth t is flat. Figure 5 shows the dimple arrangements along with their row distances.

Twelve kinds of dimpled engineering surfaces are designed and the detailed dimensions and arrangements are summarised in Table 2. The results of the mixed EHL analysis are also summarised in Table 2.

Figure 4 Dimple dimensions, (a) circle (b) ellipse (c) side view (see online version for colours)

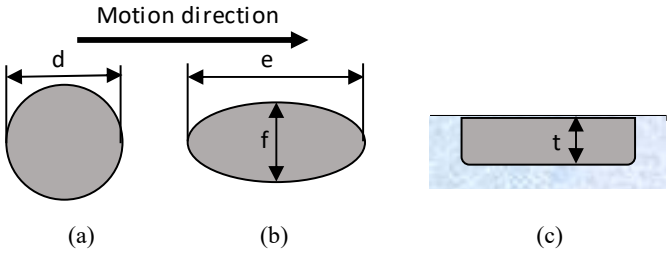

Figure 5 Dimple arrangements, (a) regular arrangements (b) zigzag arrangement

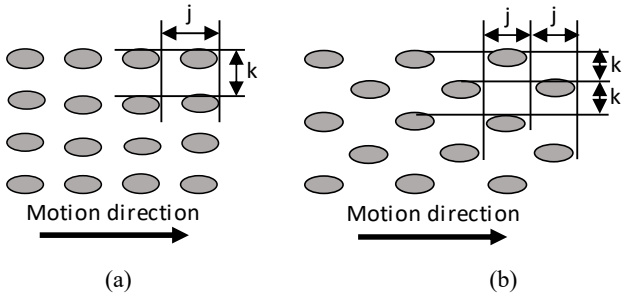

6 Results and discussion

6.1 Smooth surface solution

In Figure 1, the tested and perfectly smooth surface of body two mates with the reference surface of body one, also a perfectly smooth surface. The mixed EHL contact is simulated under the input parameters and the operating conditions described in Table 1 by applying Zhu and Hu's mixed EHL model (Zhu and Hu, 1999, 2001; Hu and Zhu, 2000; Liu et al., 2006).

Figures 6(a) and 6(b) show the film thickness and pressure distributions in the x and y directions, respectively, of the elliptical contact zone described in Figure 1(b). The central film thickness at the centre of or near the Hertzian contact is 239.5 nm and the minimum film thickness is 124.0 nm.

Figure 6 Film thickness and pressure distributions in Hertzian contact zone on perfectly smooth surface, (a) x direction (b) y direction (see online version for colours)

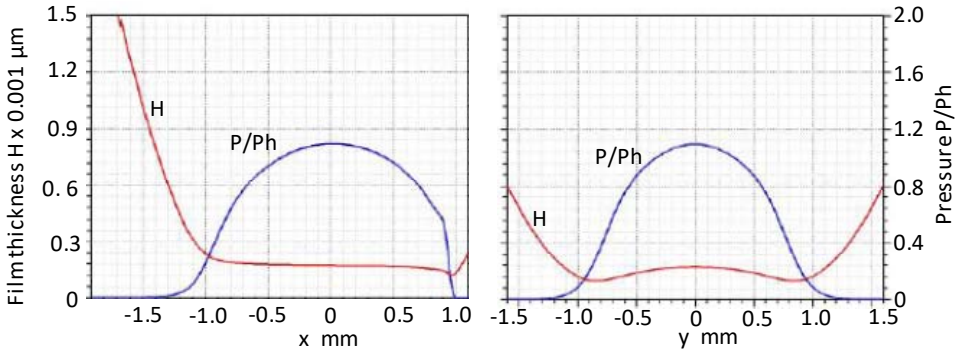

(a) (b)

6.2 *Dimpled engineering surface solutions*

Twelve kinds of dimpled surfaces are designed as body two. The dimpled engineering surfaces mate with the reference body one. The mixed EHL film thickness and the pressure distributions are simulated.

Figure 7 Case 5 solution, (a) x (entraining) direction (b) y direction (see online version for colours)

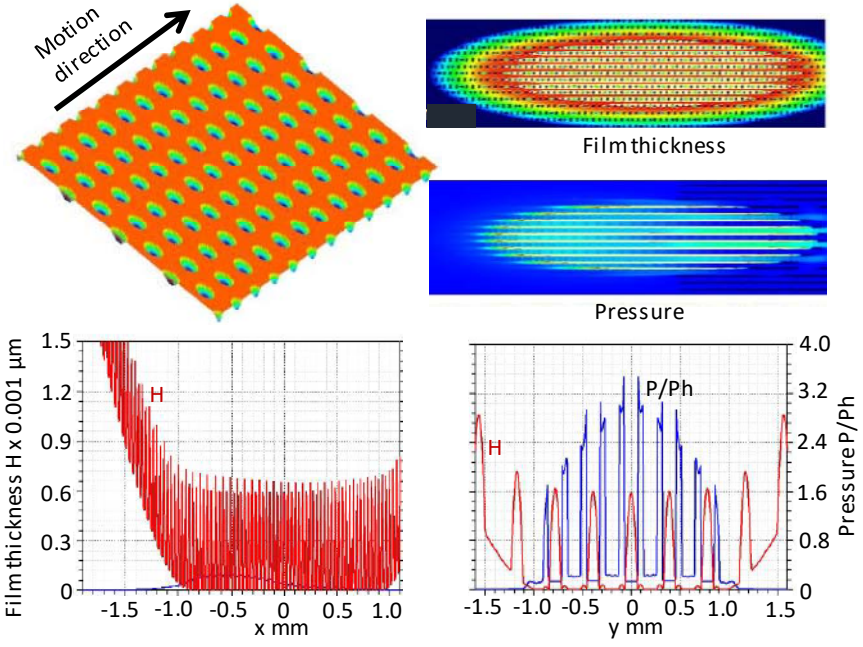

(a) (b)

Note: Average film thickness: 127.7 nm; contact load ratio: 0.358.

Figure 7 shows an image of the dimpled surface of case 5 with the motion direction and the visual images of the film thickness and the pressure distributions in the Hertzian contact zone. Graphs of the detailed simulation results of the EHL film thickness and pressure distribution in both the x (entraining) and y directions are also shown in Figure 7. In the x direction, a small amount of pressure is built up. In the y direction, several sharp spikes with high levels of pressure appear and their valleys correspond to the dimple locations. Case 5 exhibits an average film thickness of 127.7 nm and a contact load ratio of 0.358. The case 5 surface dimples appear in the zigzag arrangement and the area ratio is 26.2%.

Figure 8 demonstrates the simulation results for the dimpled surface of case 7. The dimple shape and size are the same as case 5. However, in case 7, the surface appears in the regular arrangement and the dimple area ratio is 6.6%, which is lower than that of case 5 (26.2%). In the x (entraining) direction, high pressure along the Hertzian contact is built up and the case 7 dimpled surface is completely separated from the reference surface (body one). In the y direction, high pressure also is built up – but without the sharp spikes of case 5 – and a uniform film thickness can be seen. The case 7 average film thickness is 288.4 nm, much greater than the thickness of case 5. The film thickness of case 7 is greater than that of the perfectly smooth surface case (239.5 nm). As this dimpled surface completely separates, the contact load ratio becomes zero.

Figure 8 Case 7 solution, (a) x (entraining) direction (b) y direction (see online version for colours)

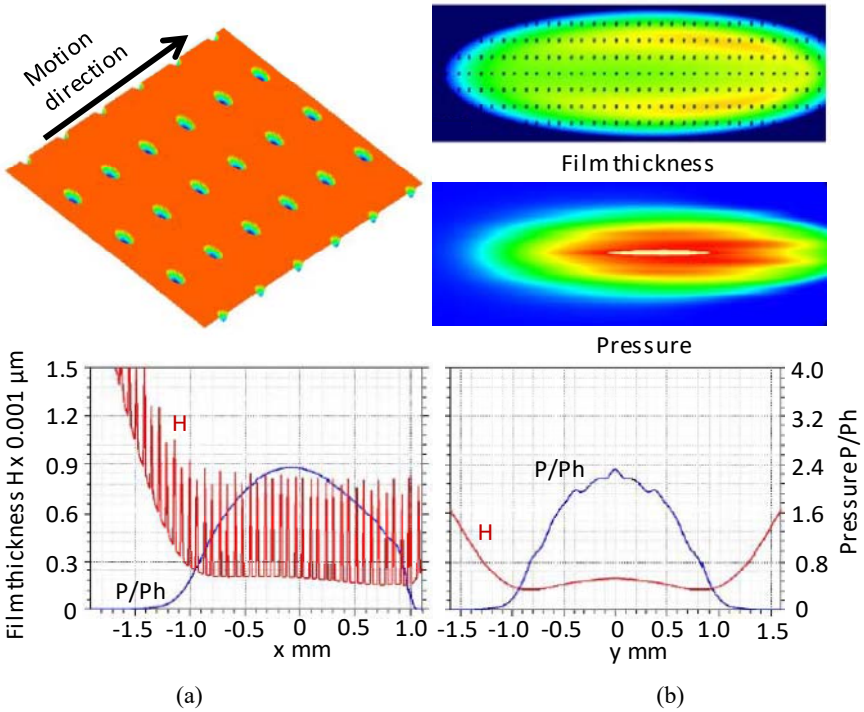

(a) (b)

Note: Average film thickness: 288.4 nm; contact load ratio: 0.

The simulation results for case 10 are shown in Figure 9. The dimple shape and orientation are similar to those of cases 5 and 7, but the size of the dimple is greater than that of cases 5 and 7. The dimple arrangement is a regular one, just as in case 7 rather than the zigzag arrangement of case 5. The dimple area is 26.2% – the same as that of case 5, but much greater than case 7 (6.6%). In the x and y directions, the pressure build up pattern can be clearly seen, as can the pressure's spiked fluctuations. The average film thickness is 167.8 nm, which is slightly greater than case 5's but much thinner than case 7's thickness. The contact load ratio is 0.124, a very small value and close to that of the separation condition.

Figure 10 summarises the mixed EHL film analysis results of the 12 dimpled surfaces compared to the perfectly smooth surface. The dimpled surfaces of cases 7 through 12 (with the exception of case 10) exhibit greater film thickness than the others and have dimple areas smaller than or equal to 6.6%. There is no clear difference in film thickness between the regular and zigzag dimple arrangements, but the orientation of the ellipse dimple seems to make a difference. A thicker film seems to develop when the major axis of the ellipse is perpendicular to the entraining direction. The dimpled surface of case 7 exhibits the greatest average film thickness, 288.4 nm, again significantly greater than the case of the perfectly smooth surface.

Figure 9 Case 10 solution, (a) x (entraining) direction (b) y direction (see online version for colours)

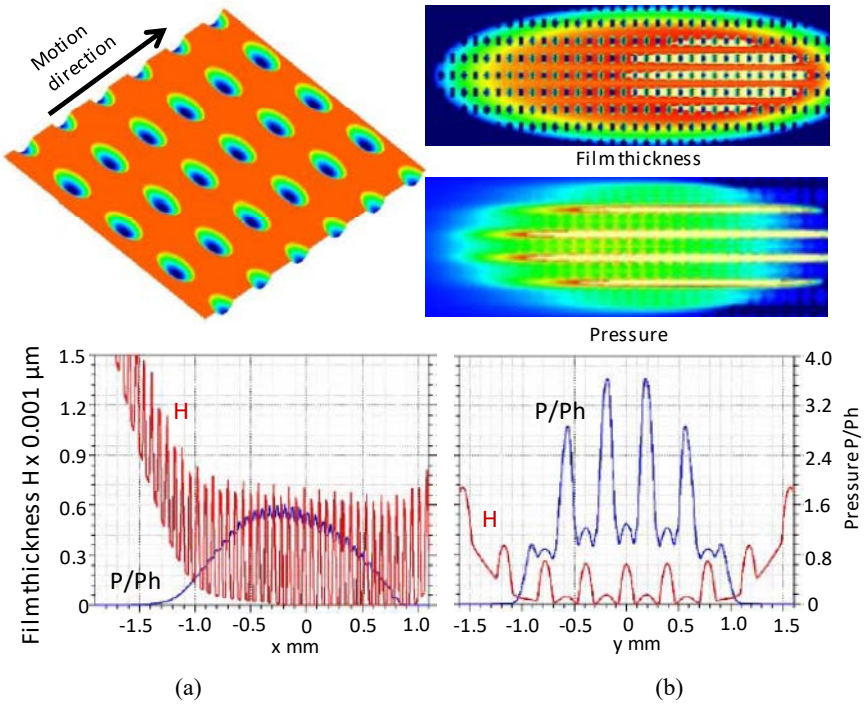

(a) (b)

Note: Average film thickness: 167.8 nm; contact load ratio: 0.124.

Figure 10 Film thicknesses of 12 different designed dimple surfaces compared to perfectly smooth surface (see online version for colours)

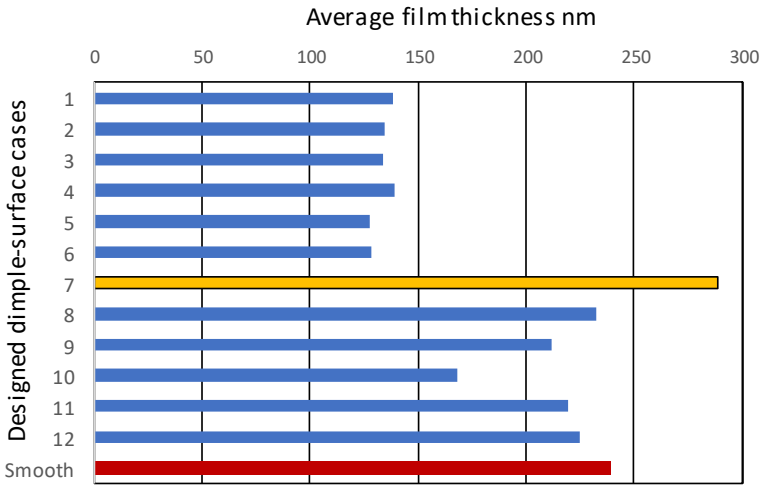

In Table 2, the contact load ratio is defined as the ratio of the load acting on the contact zone area to the total load. The λ ratio is defined as the ratio of the average film thickness to the surface roughness RMS and is used to estimate the lubrication contact performance and service life of the components. Figure 11 shows the λ ratios of cases 1 through 12. When the λ ratio is greater than 2.0, the contact load ratio becomes zero and the tested body is separated from the reference surface. Only the case 7 dimpled surfaces provides a film thickness greater than that of the perfectly smooth surface, but cases 8, 9, 11 and 12 have λ ratios greater than 2.0 – and all these dimpled surfaces exhibit greater film thickness. They are completely separated from the reference surface.

Figure 11 Film thickness vs. λ ratio compared to film thickness of perfectly smooth surface (see online version for colours)

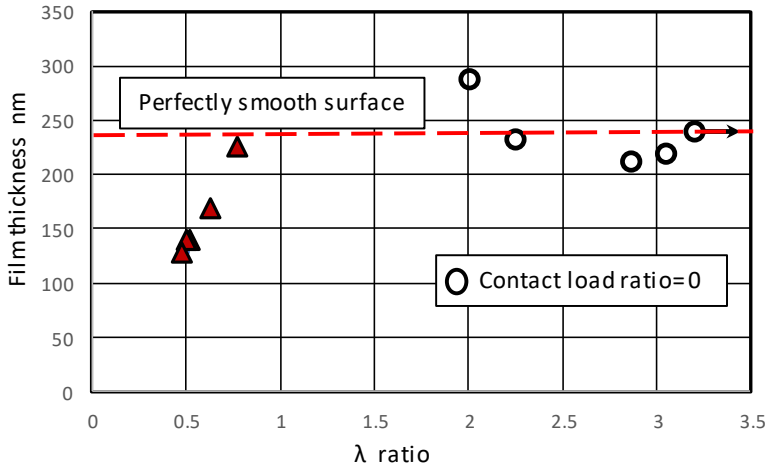

7 Conclusions

This study investigated whether introducing surface structuring technology via the fabrication of engineering surfaces with micro-patterns on their functional surfaces could achieve superior performance in critical mechanical components. Test samples with designed engineering surfaces were created with the photolithography and chemical etching methods. Twelve different dimpled engineering surfaces were designed with various dimple sizes, arrangements, dimple areas, etc. The EHL performance of a group of the designed dimple surfaces was analysed in terms of the average film thicknesses and pressure distributions in the elliptical Hertzian contact zone. In this paper, the effect of the design parameters on the lubrication performance is discussed. Also, the design criteria of dimpled engineering surfaces are discussed.

The study shows that an optimum dimpled engineering surface provides lubrication performance superior to that found in conventional machined surfaces and the film thickness of the optimum designed surface contact can be even greater than that of a perfectly smooth surface contact.

References

Dowson, D. and Higginson, G.R. (1966) *Elastohydro-dynamic Lubrication*, Pergamon Press.

Evans, C.J. and Bryan, J.B. (1999) ‘‘Texture’ or ‘engineered’ surface’, *Annals of the CIRP*, Vol. 48, No. 2, pp.541–556.

Hashimoto, F., Chaudhari, R.G. and Melkote, S.N. (2016a) ‘Characteristics and performance of surfaces created by various finishing methods’, *3rd CIRP Conference on Surface Integrity, Procedia CIRP 45*, pp.1–6.

Hashimoto, F., Yamaguchi, H., Krajnik, P., Wegener, K., Chaudhari, R., Hoffmeister, H-W. and Kuster, F. (2016b) ‘Abrasive fine-finishing technology’, *CIRP Annals – Manufacturing Technology*, Vol. 65, No. 2, pp.597–620.

Hu, Y. and Zhu, D. (2000) ‘A full numerical solution to the mixed lubrication in point contacts’, *ASME Journal of Tribology*, Vol. 122, pp.1–10.

Liu, Y., Wang, Q., Hu, Y., Wang, W. and Zhu, D. (2006) ‘Effect of differential schemes and mesh density on EHL film thickness in point contacts,’ *Journal of Tribology*, Vol. 128, pp.641–653.

Patir, N. and Cheng, H.S. (1978) ‘An average flow model for determine effects of three dimensional roughness on partial hydrodynamic lubrication’, *ASME Journal of Lubrication Technology*, Vol. 100, pp.12–17.

Zhou, R.S. and Hashimoto, F. (1995) ‘A new rolling contact surface and ‘no run-in’ performance bearings’, *Journal of Tribology*, Vol. 117, pp.166–170.

Zhu, D. and Hu, Y.Z. (1999) ‘The study of transition from full film elastohydrodynamic to mixed and boundary lubrication’, *The Advanced Frontier of Engineering Tribology*, pp.150–156, STLE.

Zhu, D. and Hu, Y.Z. (2001) ‘A computer program package for the prediction of EHL and lubrication characteristics, friction, subsurface stresses and flash temperatures based on measured 3D surface roughness’, *Tribology Transactions*, Vol. 44, pp.383–390.